HIGH-ORDER COMPOSITE BULK ACOUSTIC RESONATORS

Gavin K. Ho, Reza Abdolvand, and Farrokh Ayazi
School of Electrical and Computer Engineering, Georgia Institute of Technology
gavinho@ece.gatech.edu (404)944-6009, ayazi@ece.gatech.edu (404)894-9496

ABSTRACT

In this article, we present lateral and thickness mode low-impedance UHF resonators to obtain dispersed-frequency devices simultaneously on a single substrate. The low-impedance is enabled by using high-order modes of resonators consisting of a piezoelectric transduction film on an underlying silicon layer. The impedance of these devices reduces as mode number increases. This is attributed to the increase in transduction area. The lowest measured impedance is 55Ω at 373MHz. Resonators with 373MHz and 640MHz lateral modes and 2.5GHz thickness modes from the same substrate are presented.

INTRODUCTION

With increasing demand for higher level of integration in existing electronic systems and emerging applications, alternatives to bulky frequency selective components and resonant sensors are necessary. Micromechanical resonators are choice candidates owing to their small size and ease of integration. Several demonstrations of capacitively-transduced, silicon micromechanical resonators with high Q have been demonstrated [1,2]. Typical capacitive UHF resonators require large polarization voltages and ultra-thin electrode-to-resonator gap spacing [1] to achieve motional impedances (R_1) less than 1kΩ. These two requirements pose additional demands on resonator fabrication and interface circuits. In contrast, piezoelectric resonators can be fabricated with relative ease using low temperature processes [3–6] and have lower R_1 due to greater coupling.

Examples of piezoelectric resonators include quartz crystal units, surface acoustic wave (SAW) resonators and thin-film bulk acoustic resonators (FBAR). The main drawbacks of crystal units and SAW devices are their bulky size and incompatibility for microelectronic integration. On the other hand, FBARs can be integrated with on-chip electronics and have been demonstrated at GHz frequencies [7,8]. Since FBARs utilize the thickness vibration of a thin film, obtaining multiple dispersed frequency standards on a single substrate is challenging.

This article presents UHF composite piezoelectrically-transduced single-crystal-silicon (SCS) resonators operating in lateral bulk acoustic modes to alleviate the aforementioned constraints. The distinctiveness lies in the use of a thin-film piezoelectric solely for transduction of a silicon resonator. A high order composite bulk acoustic resonator (CBAR) is shown in Figure 1. The CBAR consists of a frequency-define silicon structure and a two-metal plus piezoelectric film transduction stack. Although the CBAR resembles the interdigitated layout of a SAW transducer, its mode is in bulk acoustic form. The term "bulk" is used to signify energy storage in the bulk of the structure, instead of the definition that the mode is present in a bulk material.

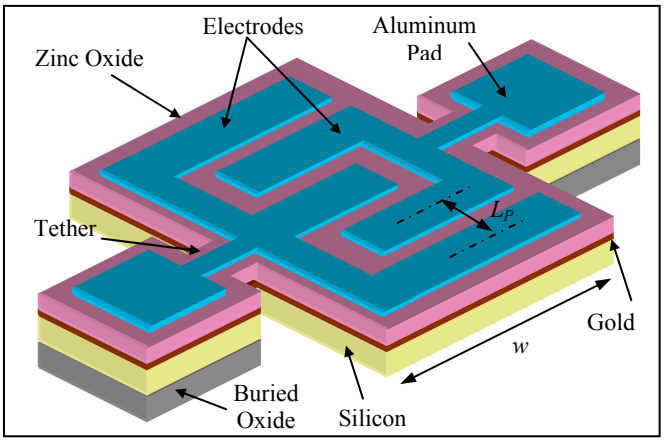

Figure 1: Composite piezoelectric-on-silicon micro-mechanical bulk acoustic resonator

There are several advantages of utilizing silicon as a structural material. The properties of SCS are stable and well-characterized to enable design for manufacturability. In addition, SCS has low acoustic loss and an energy density much greater than that of quartz [9] for high Q and good linearity. The anisotropic properties of silicon provide clean mode shapes that lead to good piezoelectric coupling for low R_1. Silicon also provides increased structural integrity to enable large suspended CBARs as in Figure 2.

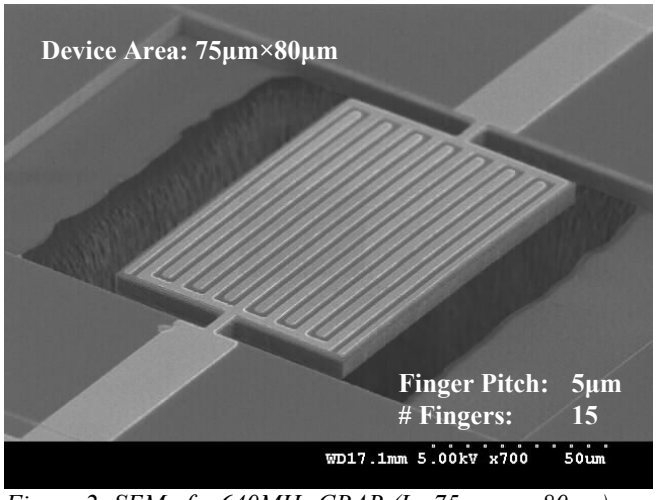

Figure 2: SEM of a 640MHz CBAR (L=75µm, w=80µm)

FABRICATION

The current CBAR fabrication process requires five masks (Figure 3). In contrast to our previous work [6], the SOI substrate may be high-resistivity since a bottom metal electrode is utilized. First, the electrode consisting of a 100Å chromium adhesion layer and a 1000Å gold film are evaporated and patterned. Next, a 0.5-1μm thick zinc oxide film is sputtered. Gold was selected for the bottom electrode because it provided the best ZnO film. Next, a 1000Å aluminum film is evaporated and patterned as the top electrode. Openings are etched into the ZnO to access the bottom metal plane. Afterwards, the device structure is defined by etching through ZnO and device silicon. Then, backside etching of the silicon and buried oxide is performed to release the structure. Using this process, devices with large planform area can be realized. An SEM of a 75μm×80μm CBAR is shown in Figure 2.

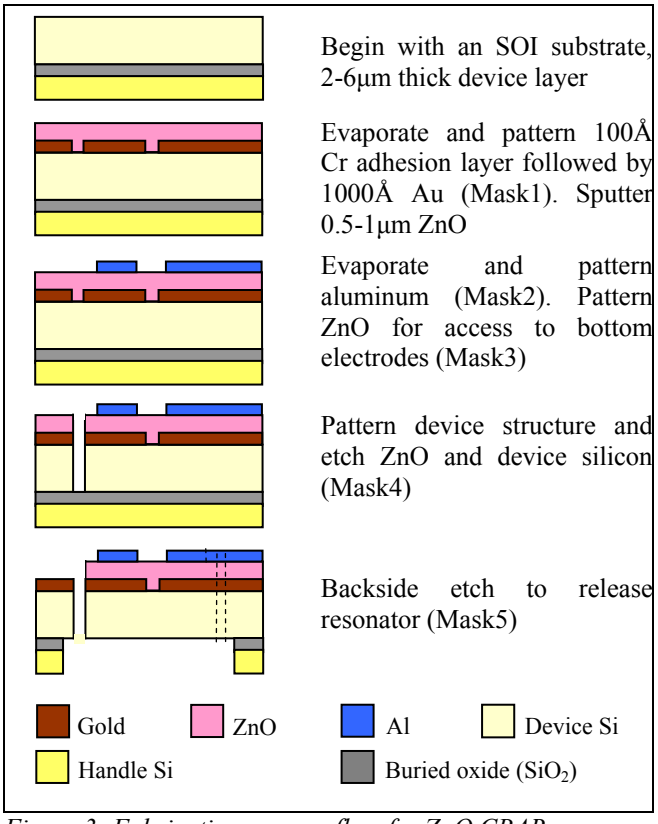

Figure 3: Fabrication process flow for ZnO CBARs

FUNDAMENTAL MODE CBARS

Our first demonstrations of composite bulk acoustic resonators (CBAR) were beams [3] and plates that showed equivalent resistances less than 2kΩ [4]. The fundamental mode plate shown in Figure 4 has a resonance at 90.4MHz with a Q of 4000 (Figure 5). This CBAR has good linearity as the 1dB compression point occurs for a 10dBm input. The motional impedance of this device is 450Ω. Similar structures incorporating the low-loss SCS exhibited quality factors up to 12000 in low vacuum [10].

From the electrical-equivalent model of the fundamental-mode CBARs, the motional resistance is,

$$R_1 \approx \frac{\pi\left(t_{Si}+t_f\right)\sqrt{E_i\rho}}{2d_{31}^{\ 2}E_f^{\ 2}wQ}$$

where t_{Si} and t_f are the thickness of the device layer and piezoelectric film, respectively, E_i and ρ are the directional elasticity and mass density of silicon, d_{31} and E_f are the piezoelectric constant and elasticity of the piezoelectric film, w is the width of the electrode (normal to the direction of motion), and Q is the quality factor. Of particular interest is the length (and frequency) can be changed without affecting R_1.[1] To reduce R_1, the easiest solution is to increase the electrode width w.

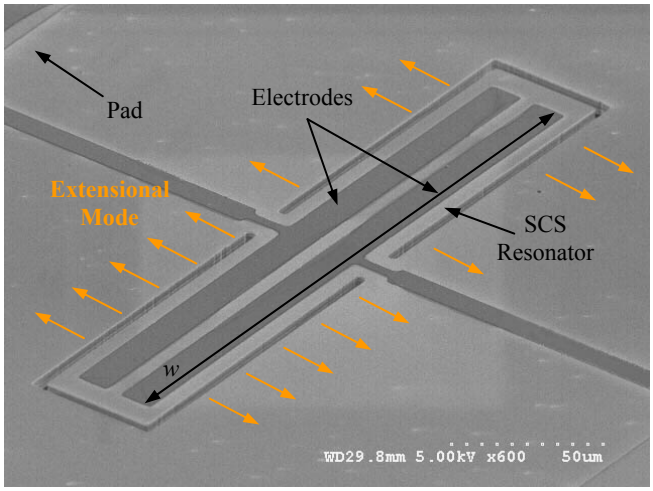

Figure 4: SEM of a 240μm×40μm fundamental-mode CBAR

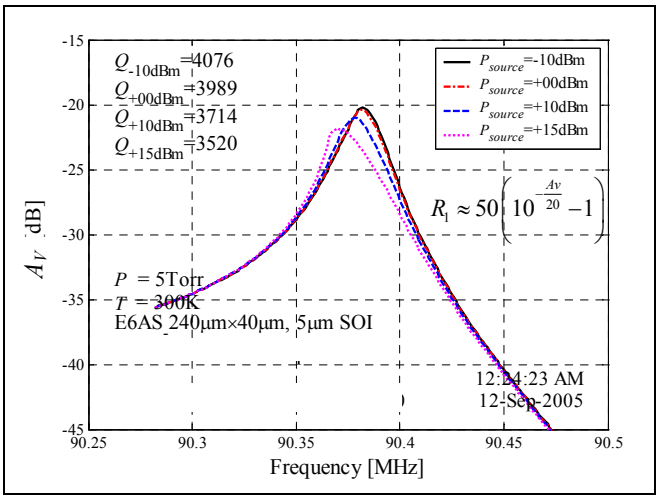

Figure 5: Linearity of a fundamental width-mode CBAR, Q=4000. P_{1dB} = 10dBm.

HIGH-ORDER MODE CBARS

High-order modes are presented for further reduction in R_1 for RF applications. For an n^{th}-mode device, the transduction area is increased by a factor of n. The structure

[1] assuming Q remains constant

in Figure 1 can be considered as a 5th-mode resonator or simply a resonator that is folded over five times. The simulated mode-shape in Figure 6 shows the regions with in-phase stress. Coupling efficiency is also determined by the mode shape. For an ideally-coupled resonator, the motional impedance is

$$R_1 \approx \frac{n}{n^2-1}\frac{\pi\left(t_{Si}+t_f\right)\sqrt{E_i\rho}}{2d_{31}^{\ 2}E_f^{\ 2}wQ}$$

for odd n, when n>1. In addition to lower R_1, a high-order mode resonator provides improved dimensional control. The frequency sensitivity to process variations is reduced by a factor of n in an n^{th}-mode resonator.

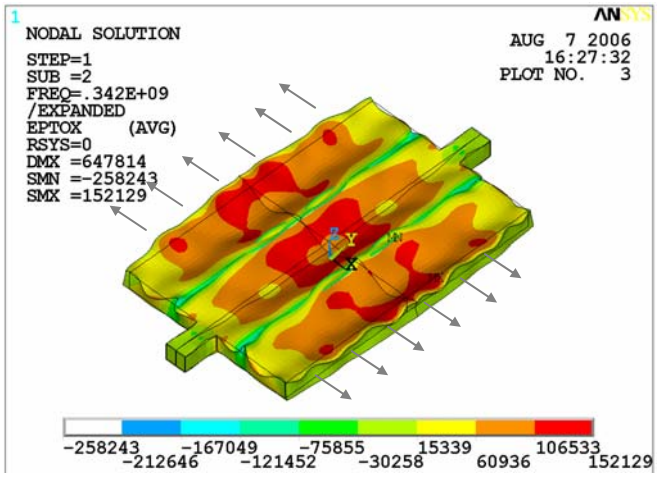

Figure 6: Simulated mode shape of a fifth-order ZnO-on-SCS CBAR with a finger pitch of 10μm

The CBAR shown in Figure 7 is an exemplary device fabricated with the five mask process. It has a finger pitch of 10μm and has lateral dimensions of 90μm×160μm. With silicon providing structural integrity, devices wider than 300μm were fabricated without stress-related issues.

Resonators were tested on a Suss RF probe station with an Agilent E5071B network analyzer at atmospheric pressure. SOLT calibration was performed with GSG probes. Two-port *s*-parameter measurements were taken, from which the motional impedance is

$$R_1 \approx 2 \cdot R_L\left(\frac{1}{s_{21}}-1\right)$$

where R_L is the termination impedance.

The 9th-mode CBAR in Figure 7 has a resonance frequency of 373MHz and exhibited an unloaded quality factor of 2000 at 1atm. See Figure 8. Higher Q is expected at lower pressures. To measure unloaded Q, the port conversion feature of the E5071B was utilized to simulate a termination of 0.5Ω. The insertion loss of 35dB at resonance corresponds to a 55Ω device impedance. This is also verified by the 35dBΩ impedance measurement (Figure 9). The isolation level of 30dB and the linear response with 10dBm input are also remarkable.

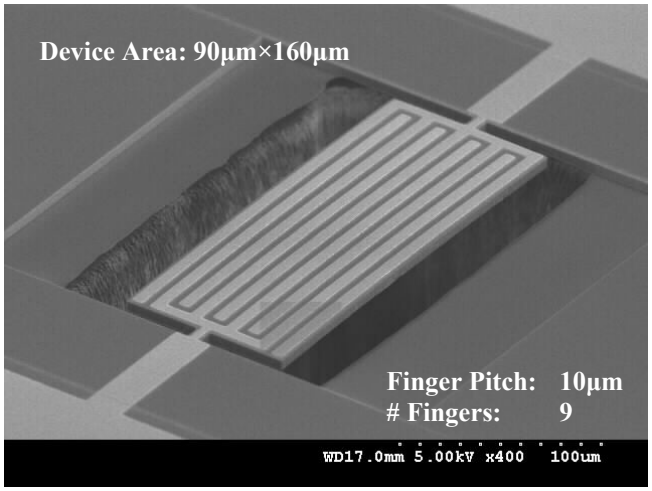

Figure 7: SEM of a 90μm×160μm CBAR with L_P=10μm

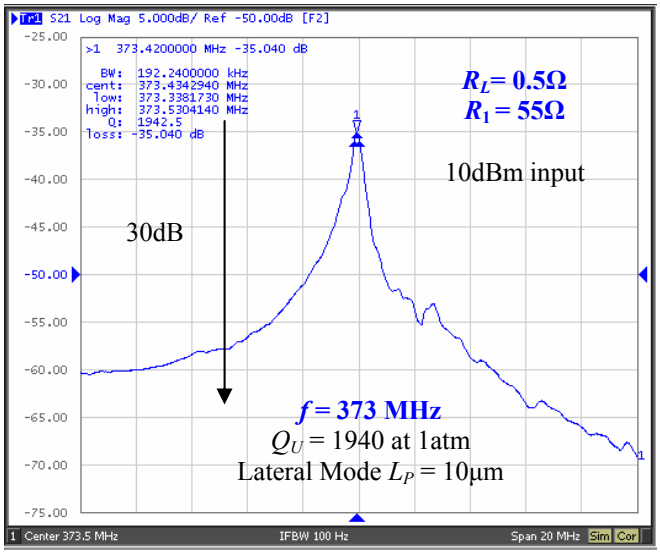

Figure 8: Freq. response of a 9th mode resonator with L_P=10μm at 1atm

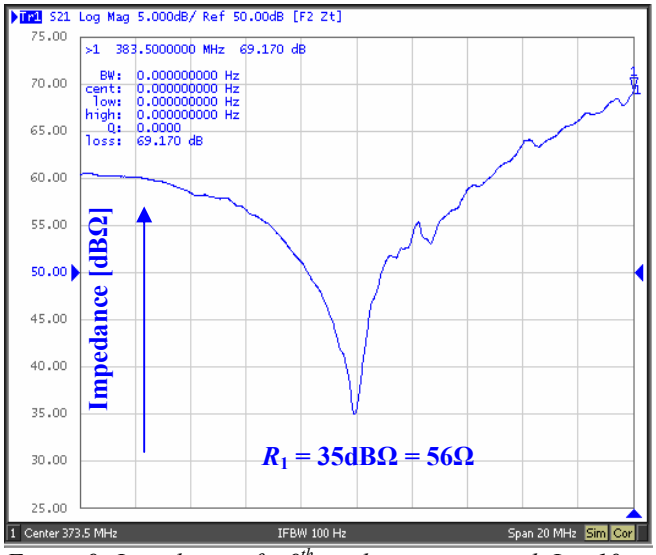

Figure 9: Impedance of a 9th mode resonator with L_P=10μm at 1atm [dBΩ]

To enable higher frequency resonators, the finger pitch is reduced. A 75μm×80μm CBAR with L_P=5μm is shown in Figure 2. Its resonance frequency is 640MHz and its impedance is 400Ω (Figure 10). Again, a linear response was observed for a 10dBm input. The reduced Q of 740 (at atmospheric pressure) is primarily attributed to anchor losses. As the frequency and the number of electrode fingers are increased, the importance of optimizing the structure for a clean mode is escalated.

One attractive feature of the presented work is the ability to fabricate thickness mode resonators next to the lateral CBAR. A small composite thickness mode resonator exhibited resonance at 2.5GHz and quality factors of 1200 (Figure 11). Although the 1kΩ impedance of the resonator is quite high, greater than 30dB isolation is observed again. With a proper design of the thickness mode resonator, good out-of-band rejection filters could be enabled. An importance aspect of piezoelectric resonator design is mode isolation. Non-optimized lateral mode CBARs will show multiple peaks, corresponding to unintended extensional modes, flexural modes, and also thickness modes.

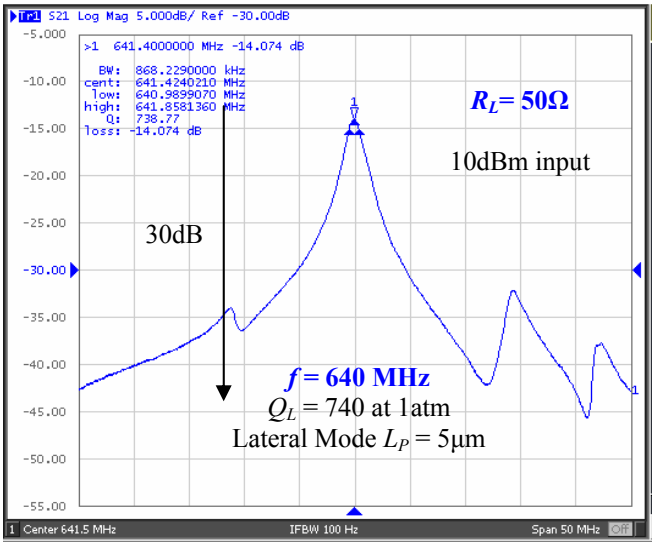

Figure 10: Frequency response of a 15th mode resonator with L_P=5μm at 1atm

CONCLUSIONS

The presented technology offers a multi-standard single-chip solution by complementing film bulk acoustic resonator technology. It is conceivable that combinations of filters for DVB, GSM, and WCDMA could be implemented on the same chip in a post-CMOS process.

ACKNOWLEDGEMENTS

This work was supported under the DARPA NMASP program. The authors thank the staff at the Georgia Tech Microelectronics Research Center for their assistance.

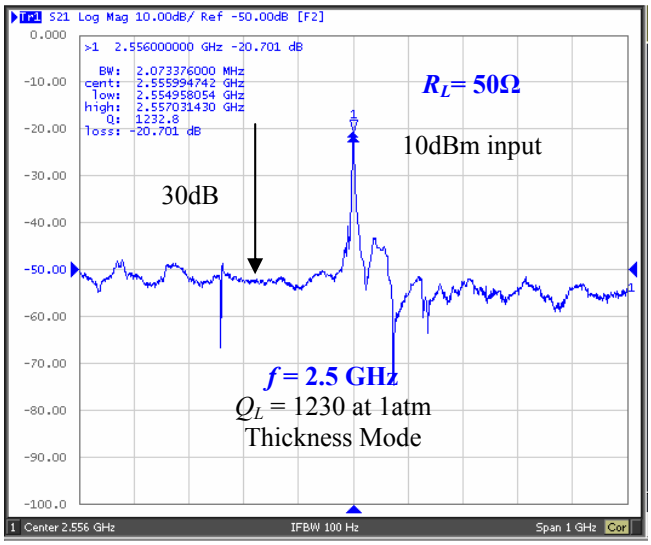

Figure 11: Frequency response of a thickness mode resonator fabricated on the same substrate as the CBARs

REFERENCES

[1] S. Pourkamali, G. K. Ho, and F. Ayazi, "Vertical Capacitive SiBARs," *MEMS2005*, pp.211-214.

[2] J. R. Clark, W.-T. Hsu, C.T.-C. Nguyen, "High-Q VHF micromechanical contour-mode disk resonators", *IEDM 2000*, pp. 493-496.

[3] G. Piazza, R. Abdolvand, G. K. Ho, and F. Ayazi, *Sensors and Actuators A*, V111, Mar. 2004, pp.71-78.

[4] S. Humad, R. Abdolvand, G. K. Ho, and F. Ayazi, "High Frequency Micromechanical Piezo-On-Silicon Block Resonators," *IEDM* 2003, pp. 957-960.

[5] S. Trolier-McKinstry and R. Muralt, "Thin film piezoelectrics for MEMS," *Journal of Electroceramics*, V12, pp. 7-17, 2004.

[6] G. Piazza, P. J. Stephanou, J. M. Porter, M. B. J. Wijesundara, and A. P. Pisano, "Low motional resistance ring-shsped contour-mode aluminum nitride piezoelectric micromechanical resonators for UHF applications," *MEMS* 2005, pp. 20-23.

[7] R. Ruby, P. Bradley, J. Larson III, Y. Oshmyansky, D. Figueredo, "Ultra-miniature high-Q filters and duplexers using FBAR Technology", *ISSCC* 2001, V44, pp. 121-122.

[8] K. M. Lakin, "Thin film resonator technology," *IEEE Trans. UFFC*, V52 N5, pp. 707-716, May 2005.

[9] V. Kaajakari, T. Mattila, A. Oja, and H. Seppa, "Nonlinear limits for single-crystal silicon microresonators," *JMEMS*, V13 pp.715-724, Oct.2004.

[10] F. Ayazi *et al*, "High Aspect-Ratio SOI Vibrating Micromechanical Resonators and Filters," *IMS2006*, pp. WE2G-4